Overmodulation Strategy for High-Performance Torque Control

Jul-Ki Seok, *Student Member, IEEE*, Joohn-Sheok Kim, *Member, IEEE*, and Seung-Ki Sul, *Member, IEEE*

***Abstract*—In the overmodulation region, the operation of the electrical drive system with a current controller is characterized by a rapid deterioration of motor torque and speed. It is desirable to use the overmodulation strategy, which guarantees the fast response even in transient state and satisfies the overall closed-loop control performance. In this paper, in order to improve the dynamic characteristics of the electrical drive, a new overmodulation technique is proposed. Considering the current transition characteristics, an efficient overmodulation strategy is introduced to achieve better transient performance through an adequate voltage selection. With the help of a new overmodulation strategy, required electrical torque can be directly produced as quickly as possible, and stable drive characteristics can be achieved in the transient condition. The proposed method has been implemented on an actual inverter system and thoroughly tested on a 900-W interior permanent magnet synchronous machine (IPMSM) to confirm its feasibility.**

***Index Terms*—Current regulation, IPMSM, overmodulation.**

I. Introduction

RECENTLY, much research effort has been spent in improving the transient torque regulation in accordance with industrial demands for higher performance drive capability [1], [2]. In the high-performance machine drive system such as spindle, traction, or robotics, fast response to the abrupt reference change and robust characteristic to the load variation are the essential requirements. In order to ensure these requirements, high-quality current regulation is the first key ingredient for achieving high-performance torque control with a sinusoidal ac machine. In general, the machine current is basically determined by the machine terminal voltage and the inherent machine-back electromotive force (EMF). Therefore, if machine-back EMF and stator current are known, it is straightforward to generate electronically terminal voltage within the inverter by using pulsewidth modulation (PWM) [3]. When a current-controlled PWM is used, a conventional PWM voltage-source inverter is equipped with fast current control loops. The role of the ac-current regulation is to select the correct voltage vector such that machine current will follow the desired current command. Consequently, the torque developed by the machine can be controlled directly by varying current amplitude and phase.

Manuscript received July 26, 1996; revised October 2, 1997.

J.-K. Seok is with SamSung Electronics Corporation, Suwon City, Kyungki-Do, Republic of Korea.

J.-S. Kim is with the Department of Electrical Engineering, University of Inchon, Inchon, Korea.

S.-K. Sul is with the School of Electrical Engineering, Seoul National University, Seoul, Korea.

Publisher Item Identifier S 0885-8993(98)04862-5.

However, practically, the machine terminal voltage can be generated only through the power stage including the inverter system, and the maximum output voltage is restricted by the dc-link voltage. Especially in the transient state, the overall dynamic performance of the drive system may be determined by the voltage-selection algorithm because the required machine voltage tends to exceed the voltage limit boundary provided by the actual inverter system. In this case, where the PWM inverter approaches square-wave operation, the fundamental current magnitude will be less and its phase will deviate from that of the commanded current. Thus, the performance of the torque control is highly dependent on the voltage modulation algorithm of the inverter system. So, introducing more efficient voltage-selection techniques for the overmodulation region, the transient response of the machine drive system can be significantly improved without considerable effort. From this point of view, some previous studies have been reported for the voltage-selection technique in the overmodulation region. Some of the earliest works [4]–[6] have observed the importance of designing a controller that transitions smoothly from PWM control to six-step operation, independent of the modulation strategy employed. In these techniques, the dynamic behavior of the current controller on the voltage limit boundary was not considered. Other authors [1], [7], [8] have addressed the voltage-selection algorithm on the voltage limit boundary. The reference voltage of the current regulator is composed of back-EMF voltage and dynamic voltage to minimize the current error. In [1], [7], and [8], the whole reference voltage is truncated to the hexagon boundary in the overmodulation region, and the dynamic voltage to reduce the current error is not preserved in the sense of amplitude and angle. Thus, these techniques cannot provide the enough current controllability in the overmodulation range.

In this paper, a novel overmodulation strategy for high-performance interior permanent magnet synchronous machine (IPMSM) is proposed. The current transition is determined by the difference between the machine terminal voltage and the machine-back EMF. Therefore, considering the machine-back EMF, the optimal inverter output voltage is selected in the proposed overmodulation strategy. With this algorithm, required electrical torque can be directly produced as quickly as possible and stable machine drive characteristics can be achieved in the transient condition. For the sake of actual implementation of the new overmodulation scheme, the detailed expression is also described. With this overmodulation scheme on the controller, by adding a software program, an inverter can be effectively utilized for any ac-current regulation system.

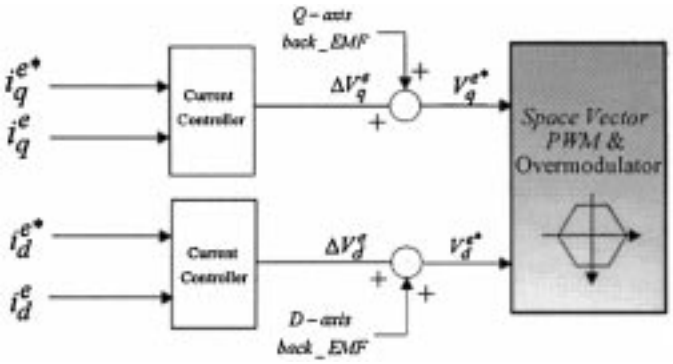

Fig. 1. Control structure with current controller.

II. General Torque Control for IPMSM

The effects of current regulation performance on torque production related to d- and q-axis currents are of fundamental interest and widely known from the IPMSM model. The torque quantity related to d–q-axis currents can be expressed on the d–q synchronous reference frame fixed to rotor angle as follows:

$$T_e = \tfrac{3}{2}P[(\psi_f i_q^e + (L_d - L_q) i_q^e i_d^e]. \tag{1}$$

In the above equation, i_d^e, i_q^e, L_d, and L_q indicate the equivalent circuit d–q-axis stator currents in the synchronous rotating reference frame and stator inductances, respectively, and ψ_f is the magnet flux. P represents the number of pole pairs. Interior permanent magnet synchronous machines possess special intrinsic feature for adjustable-speed operation which distinguish them from other classes of ac machines [9]. The rotor magnetic saliency by d–q-axis inductance difference introduces a reluctance torque term into the torque equation and the torque production in IPMSM is altered as a result of the rotor saliency. To develop the desired torque at maximum torque-per-amp, the d–q-axis stator currents simultaneously change. Therefore, the electrical torque is controlled by regulating the d–q-axis current in the desired direction.

Current regulation is often accomplished through the compensation of the synchronous motor back-EMF voltage component by the feedforward manner as shown in Fig. 1 [10], [11]. Appealing steady-state and dynamic performance characteristics can be achieved using this feedforward regulator scheme even when the values of the machine parameters are not known precisely. In Fig. 1, $\Delta\vec{V}_{qd}^{e}$ is the dynamic voltage vector which decides the transition of the current vector, and the motor back EMF is the steady-state voltage vector. For the effective torque control, when the reference voltage vector exceeds the outside hexagon, the information of $\Delta\vec{V}_{qd}^{e}$ corresponding to the current dynamics should be kept as much as possible.

The maximum output voltage of the actual inverter system is restricted by the dc-link voltage. According to the space-vector theory [12], the maximum magnitude of the voltage vector which can be applied to the machine is $(2/3)V_{dc}$, and the limit line of the voltage magnitude has the hexagon shape in the stationary reference frame. In order to guarantee the linearity of the inverter output voltage, the reference vector should be given within the hexagon area. However, the reference voltage calculated by the inner loop controller tends to exceed this voltage limitation when the torque reference provided by the outer loop controller is suddenly changed to satisfy the desirable overall closed-loop control performance. This phenomenon comes into account frequently in the transient condition such as the case of speed command change or load variation.

III. Overmodulation Strategy

A. Conventional Strategies

A simple way of decision to redefine the voltage vector is that the magnitude of the original vector will be limited at point a of the hexagon surface as shown in Fig. 2(a). In this conventional overmodulation strategy a, a newly modified vector can be simply obtained using the d–q component ratio between the original and modified vectors [1]. However, this modified vector determined through the conventional algorithm may result in sluggish transient dynamics because consideration about the basic current transition phenomena is neglected. Therefore, if the modified vector on the point a is selected, it is quite obvious that the undesired current transition should take place since the current dynamics will be determined by the wrong vector $\Delta\vec{V}_1$. The actual inverter switching times T_1 and T_2 are simply computed from modified voltage vector using the geometrical relationship

$$T_1 = \frac{T_s}{T_1' + T_2'} T_1' \tag{2}$$

$$T_2 = \frac{T_s}{T_1' + T_2'} T_2'. \tag{3}$$

Using space-vector PWM [12], which operates in a complex plane divided in the six-switching state vectors, the switching state of the inverter is determined from the reference voltage vector. The switching state vectors are defined by combination of conducting or nonconducting switches in the power circuit of inverter. The reference voltage vector is realized in an average sense by computing the switching times T_1 and T_2 for which two adjacent switching state vectors in the complex plane are active. T_1' and T_2' are the switching times calculated from original reference voltage vector and T_s is the sampling time.

An alternative way of decision to redefine the voltage vector is that the magnitude of the original vector will be limited at the point b of hexagon surface as shown in Fig. 2(b), and a newly modified vector can be simply obtained using the d–q component difference between the original and modified vectors [7], [8]. The conventional overmodulation strategy b can smoothly transition from the linear region to six-step operation, however, this modified vector determined through the conventional algorithm may result in degradation of transient dynamics as like strategy a [13]. The actual inverter switching times T_1 and T_2 are simply computed from modified voltage vector using the geometrical relationship

$$T_1 = T_1' - \frac{T_1' + T_2' - T_s}{2} \tag{4}$$

$$T_2 = T_2' - \frac{T_1' + T_2' - T_s}{2}. \tag{5}$$

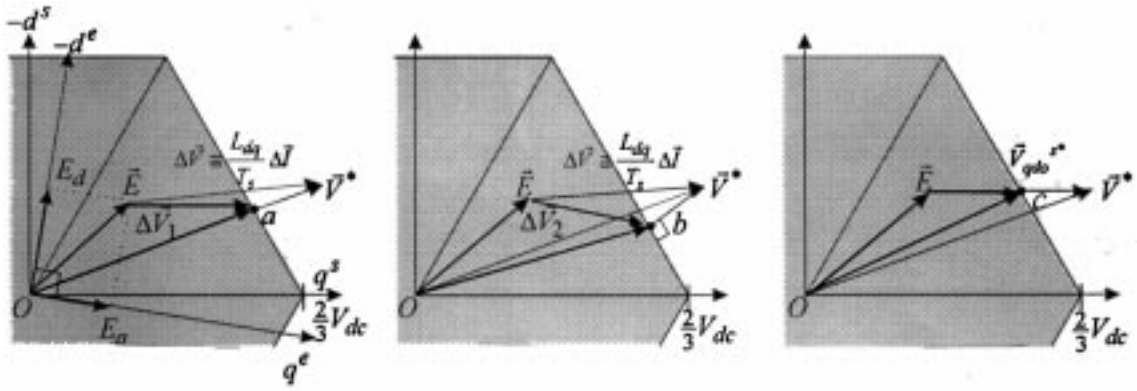

Fig. 2. Novel overmodulation scheme considering behavior of current dynamics.

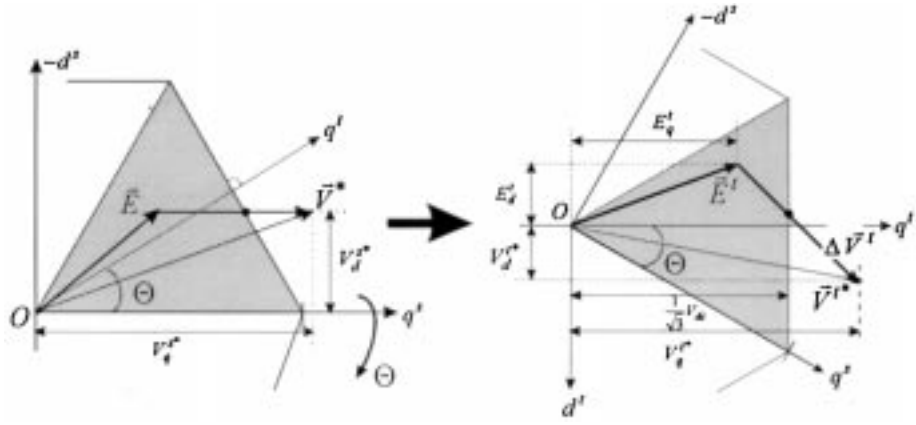

Fig. 3. Transformation from d^s–q^s frame to d^t–q^t frame.

B. New Overmodulation Method Considering Current Dynamics

As described above, the reference voltage vector generated by current controller consists of two voltage vector terms. One is the steady-state voltage vector identical to the machine-back EMF vector $\vec{E}$ and the other is the dynamic voltage vector $\Delta\vec{V}$, which decides the transition of the current vector. Assuming that the resistance voltage drop is negligible, the second term of the reference voltage vector $\Delta\vec{V}$ directly decides the dynamic behavior of the current vector. Therefore, in order to minimize the current errors considering the current transition, a new reference voltage vector $\vec{V}_{qdo}^{s^*}$ on the point c of the Fig. 2(c) should be selected. Introducing this novel voltage-selection technique for the overmodulation strategy, not only extremely fast current regulation performance in the current regulator, but also stable machine drive capability can be achieved in the transient condition.

On the other hand, at low speed, the proposed algorithm has a similar performance to the conventional strategy a because of small back EMF, i.e., the greater the back EMF is, the more effective the proposed algorithm is. Especially in the field-weakening operation region, the effectiveness of the new overmodulation strategy can be maximized. Of course, more calculation effort may be required in this advanced overmodulation strategy compared with the conventional strategies. However, using a simple reference frame conversion theory for the d–q-axis quantity such as voltage and back EMF, modified voltage vector $\vec{V}_{qdo}^{s^*}$ on the point c can be easily deduced in the proposed novel overmodulation scheme.

C. Implementation of New Overmodulation Scheme

The calculated output-voltage vector $\vec{V}^*$ in Fig. 3(a) is located on the vector space represented with the stator-fixed d^s–q^s frame. In order to easily obtain the resultant reference vector $\vec{V}_{qdo}^{s^*}$ on the hexagon boundary in Fig. 2(c), the reference vector $\vec{V}^*$ and back-EMF vector $\vec{E}$ in Fig. 3(a) are made to rotate with an angle Θ between the stator-fixed d^s–q^s frame and temporary d^t–q^t frame. The q^t axis is orthogonal to the hexagon side in each sector. In Fig. 3(a), $V_d^{s^*}$ and $V_q^{s^*}$ are the d–q-axis voltage components of the original target vector $\vec{V}^*$, respectively. In Fig. 3(b), $V_d^{t^*}$ and $V_q^{t^*}$ are the d–q-axis voltage components of rotated target vector $\vec{V}^{t^*}$. E_d^t and E_q^t represent the d–q-axis voltage components of rotated back-EMF vector $\vec{E}^t$. These rotated d–q-axis variables are simply obtained by

$$\begin{bmatrix} V_q^{t^*} \\ V_d^{t^*} \end{bmatrix} = T(\Theta)\begin{bmatrix} V_q^{s^*} \\ V_d^{s^*} \end{bmatrix} \tag{6}$$

$$\begin{bmatrix} E_q^t \\ E_d^t \end{bmatrix} = T(\Theta)\vec{E} \tag{7}$$

$$T(\Theta) = \begin{bmatrix} \cos(\Theta) & \sin(\Theta) \\ -\sin(\Theta) & \cos(\Theta) \end{bmatrix} \tag{8}$$

where $\Theta = 30° + 60°(m-1)$.

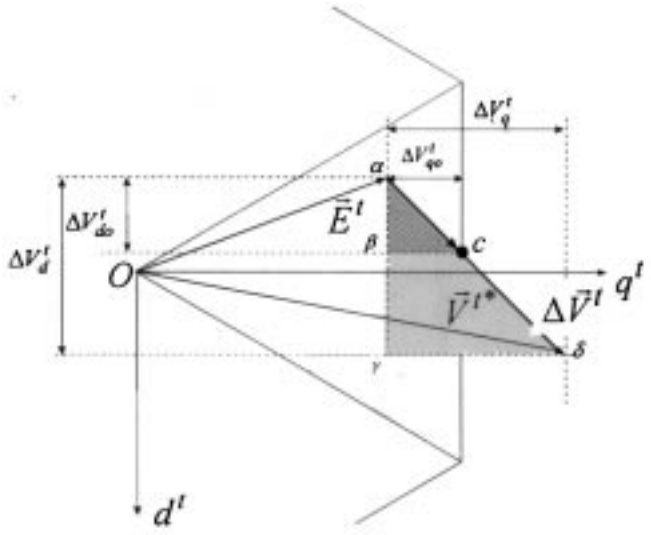

Fig. 4. Calculation of modified voltage vector in proposed strategy.

$T(\Theta)$ is a transformation matrix, and m is a sector number [12]. In Fig. 4, the difference vector $\vec{V}^t$ between rotated target vector $\vec{V}^{t^*}$ and rotated back-EMF vector $\vec{E}^t$ is composed of ΔV_d^t and ΔV_q^t. Also, it is observed that the triangles $\alpha\beta c$ and $\alpha\gamma\delta$ are similar triangles. As the two triangles are similar, then ΔV_{do}^t is simply obtained as follows:

$$\Delta V_{do}^t = \frac{\Delta V_d^t}{\Delta V_q^t} \Delta V_{qo}^t \tag{9}$$

$$\Delta V_{qo}^t = \frac{1}{\sqrt{3}} V_{dc} - E_q^t. \tag{10}$$

Now, the modified output-voltage vector $\vec{V}_{qdo}^{s^*}$ on the hexagon boundary in Fig. 2(c) is obtained by

$$\vec{V}_{qdo}^{s^*} = T^{-1}(\Theta) \begin{bmatrix} E_q^t + \Delta V_{qo}^t \\ E_d^t - \Delta V_{do}^t \end{bmatrix}. \tag{11}$$

Using space-vector PWM theory [12], the switching times T_1 and T_2 are finally computed using the modified output-voltage vector $\vec{V}_{qdo}^{s^*}$.

IV. Simulation Results

In order to verify the feasibility of the proposed IPMSM drive algorithm, digital computer simulation is carried out. A 900-W IPMSM is used in the simulation, and the ratings and parameters of IPMSM are shown in Table I. The switching device is assumed to be an insulated gate bipolar transistor (IGBT) of 5-kHz switching frequency and the dc-link voltage is 270 V considering the dead-time effect. The sampling period of current and speed control is 100 μs and 1 ms, respectively, and the inertia of the system is assumed as the value of ten times as large as the inertia of motor itself considering the load inertia, and the cutoff frequency of the current controller and speed controller is selected to 3000 and 300 rad/s, respectively.

Figs. 5 and 6 show that the speed reference is changed from 1500 to 1800 r/min at initial. In Figs. 5(a) and 6(a), the dynamic performance of the conventional overmodulation strategy and proposed control scheme are depicted, respectively. These results show that the settling time of proposed strategy is reduced by 18% compared with that of the conventional one. In Figs. 7 and 8, the speed reference is 1800 r/min, and a load torque is applied to the motor from no load to 60% of the rated load at initial. As discussed earlier, disregarding the motor dynamics, the dynamic performance is unsatisfactory, and the dipping of the machine speed is larger than that of the proposed strategy. These results are responsible for undesired current transition determined by the wrong vector $\Delta\vec{V}_1$ as shown in Fig. 2(a). It is clear from Figs. 6 and 8 that the current dynamics are quite fast during the transient state. The speed dipping of proposed strategy is reduced by 15% compared with that of the conventional one. The overall system dynamics are significantly improved under transient condition.

In the proposed strategy, the instantaneous value of the back EMF is evaluated with the knowledge of the speed, current, magnet flux, and stator inductances. It is assumed in this paper that the magnet flux and stator inductances are known

TABLE I
Ratings and Known Parameters of IPMSM Under Test

Rated power output and line voltage	900 W, 220 V
Number of pole	4
Supply frequency	60 Hz
r_s	4.3 Ω
ψ_f	0.272 Wb (at 25 °C)
L_d	27 mH
L_q	67 mH

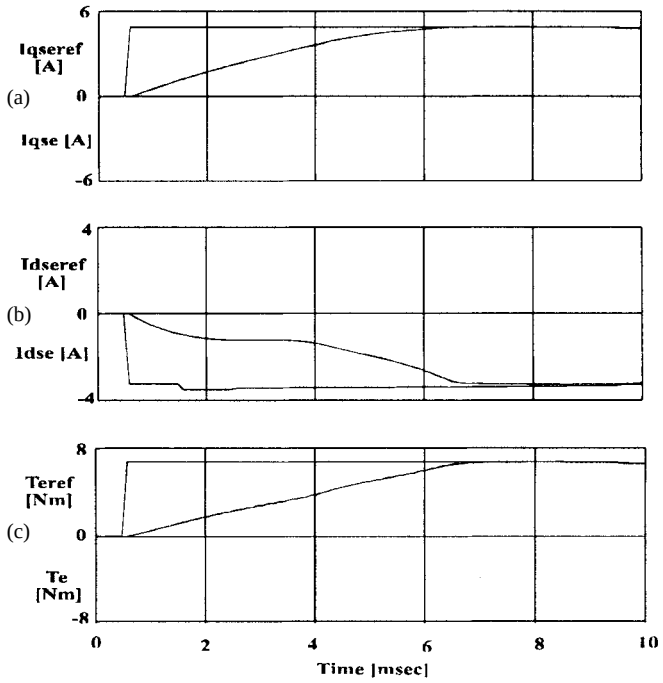

Fig. 5. Dynamic response in step speed command in the case of conventional overmodulation strategy: (a) q-axis current reference and actual current, (b) d-axis current reference and actual current, and (c) motor torque reference and actual torque.

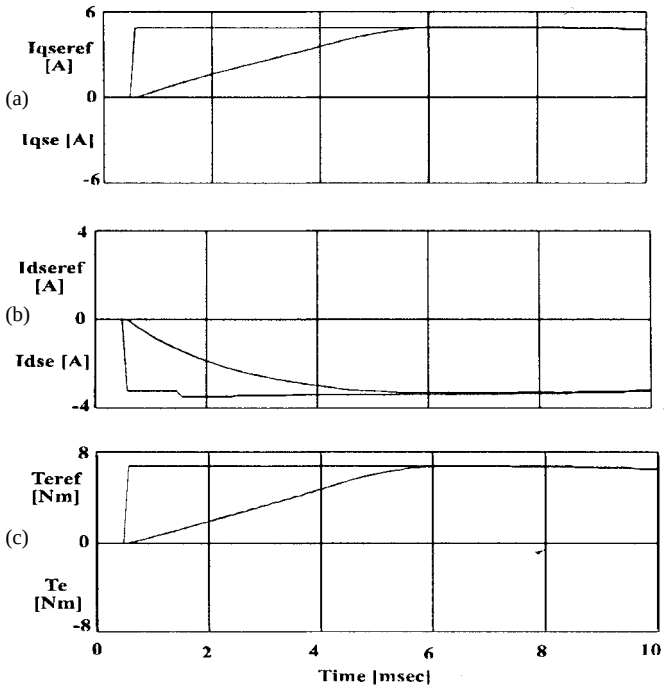

Fig. 6. Dynamic response in step speed command in case of proposed novel overmodulation strategy: (a) q-axis current reference and actual current, (b) d-axis current reference and actual current, and (c) motor torque reference and actual torque.

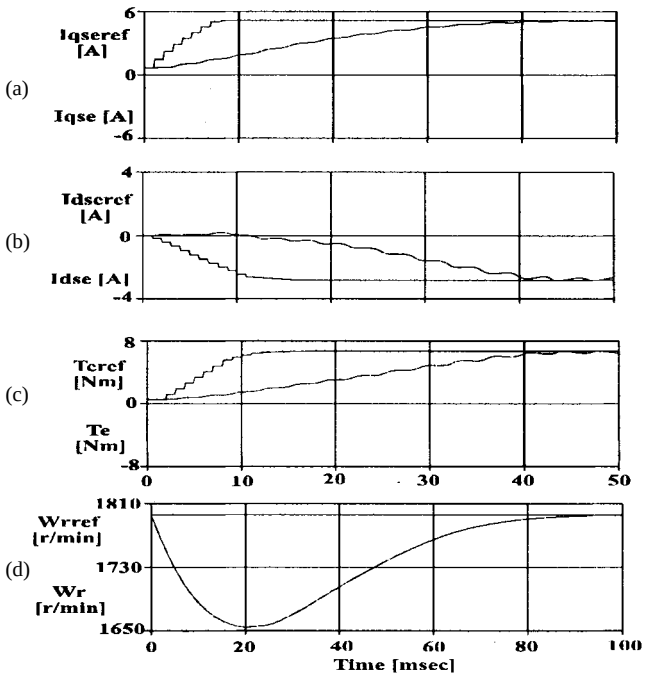

Fig. 7. Dynamic response in load change in the case of conventional overmodulation strategy: (a) q-axis current reference and actual current, (b) d-axis current reference and actual current, (c) motor torque reference and actual torque, and (d) motor speed reference and actual speed.

quantities. Thus, the d–q-axis back-EMF components can be obtained by

$$E_d^e = -\omega_r L_q i_q^e \tag{12}$$

$$E_q^e = \omega_r (L_d i_d^e + \psi_f). \tag{13}$$

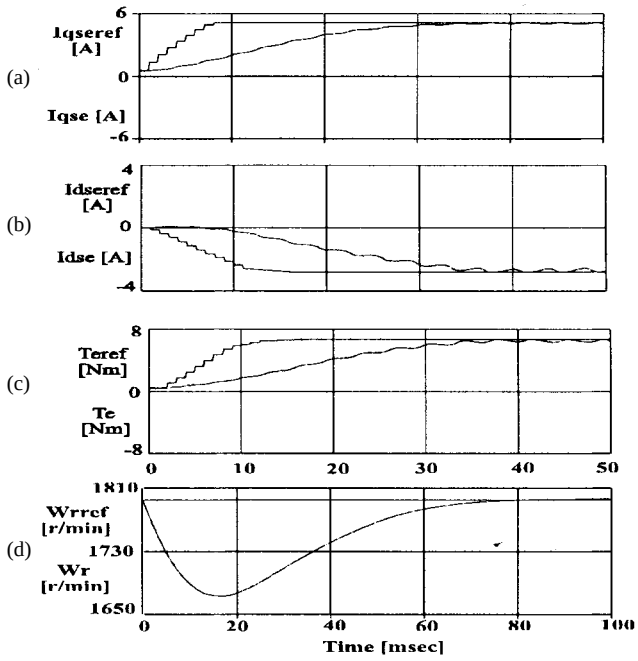

Fig. 8. Dynamic response in load change in case of proposed overmodulation strategy: (a) q-axis current reference and actual current, (b) d-axis current reference and actual current, (c) motor torque reference and actual torque, and (d) motor speed reference and actual speed.

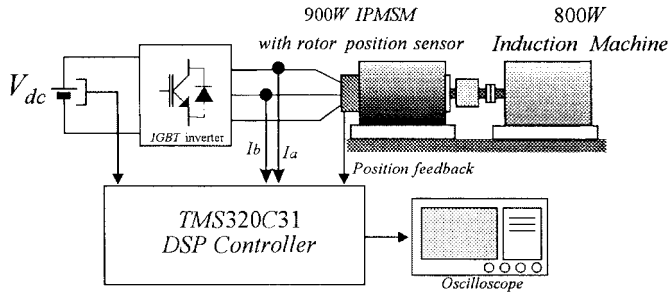

Fig. 9. Experimental system configuration.

V. Experimental Results

Extensive tests are performed to evaluate the feasibility of the presented study. The algorithm is programmed and installed on an actual IGBT inverter to drive a 900-W IPMSM coupled with an 800-W induction machine for a load test. The overall experimental setup is shown in Fig. 9. The switching devices in the inverter are IGBT's with 5-kHz switching frequency, and the dc-link voltage is 300 V. TMS320C31 digital signal processor (DSP) is used as the main control processor, and all internal data of DSP can be displayed on the oscilloscope through a multichannel 12-b digital–analog (D/A) converter.

Figs. 10 and 11 show the actual dynamic responses of step speed reference change from 1500 to 1800 r/min. From the comparison of the reference tracking performance, it is seen that the proposed strategy provides significantly improved dynamic performance. The results show that the settling time of proposed strategy is reduced by 15% compared with that of the conventional one. The responses in Figs. 10 and 11 coincide well with those in the simulation results of Figs. 5 and

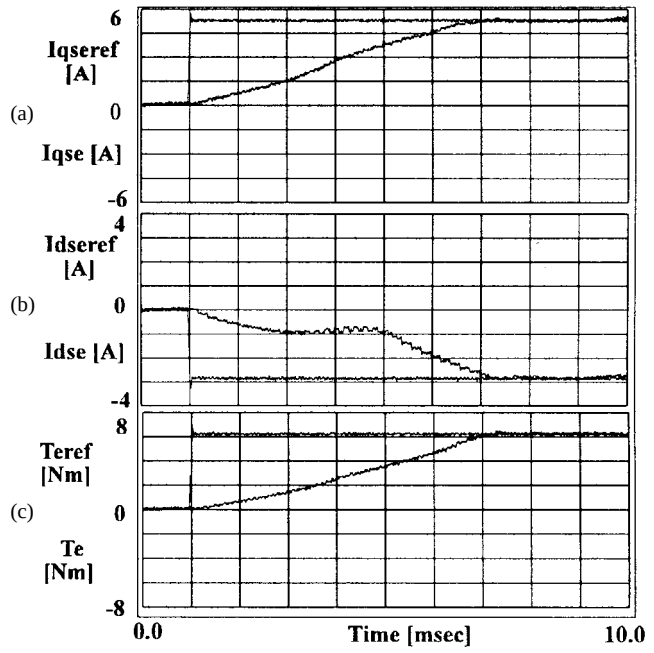

Fig. 10. Dynamic response in step speed command in the case of conventional overmodulation strategy: (a) q-axis current reference and actual current, (b) d-axis current reference and actual current, and (c) motor torque reference and actual torque.

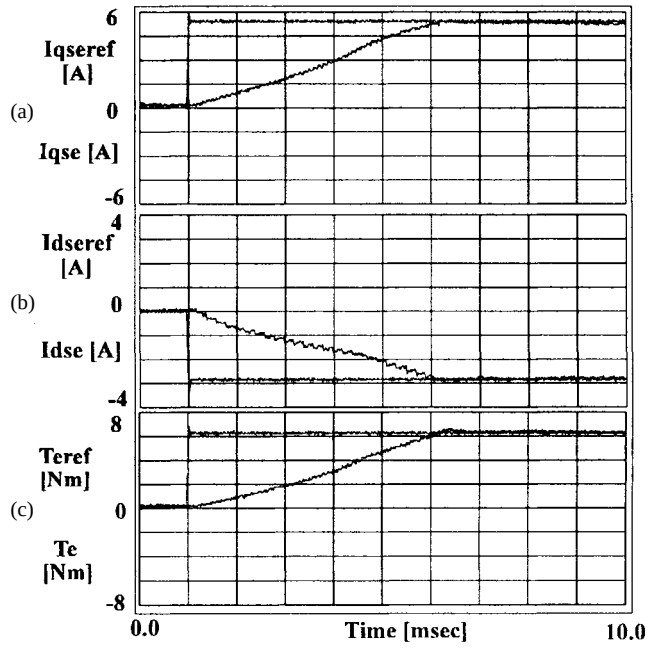

Fig. 11. Dynamic response in step speed command in case of proposed overmodulation strategy: (a) q-axis current reference and actual current, (b) d-axis current reference and actual current, and (c) motor torque reference and actual torque.

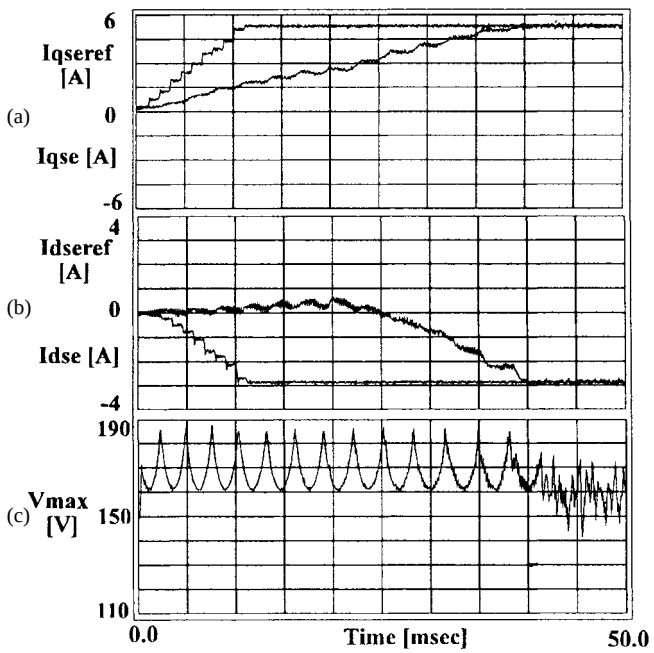

Fig. 12. Dynamic response in load change in the case of conventional overmodulation strategy: (a) q-axis current reference and actual current, (b) d-axis current reference and actual current, and (c) magnitude of controller output-voltage vector.

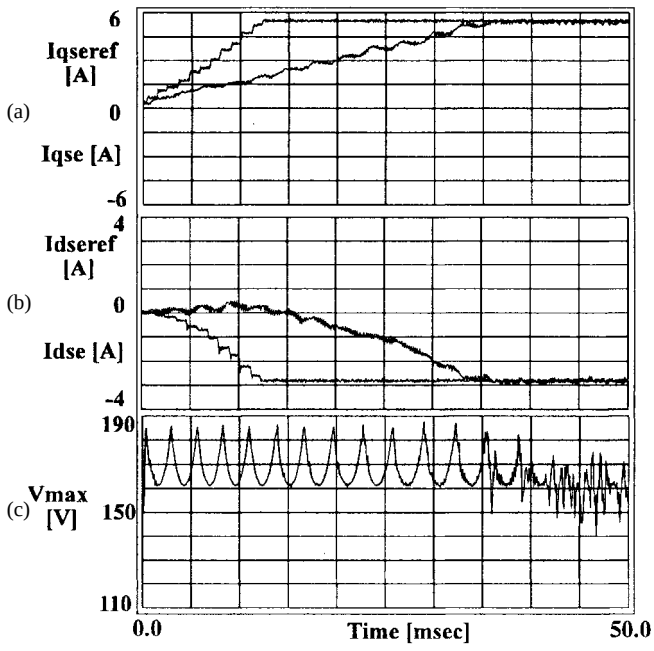

Fig. 13. Dynamic response in load change in case of proposed overmodulation strategy: (a) q-axis current reference and actual current, (b) d-axis current reference and actual current, and (c) magnitude of controller output-voltage vector.

6. In Figs. 10(c) and 11(c), the actual torque is calculated with the knowledge of measured currents and machine parameters.

To verify the effectiveness of the proposed algorithm in case of load change when the actual speed is 1800 r/min, a load torque is applied to the motor from no load to 60% of the rated load. In Figs. 12(a) and 13(a), the transient responses of the conventional overmodulation strategy and proposed control scheme are depicted, respectively. These waveforms clearly show that a machine drive capability can be increased in the transient condition by the novel voltage-selection technique for the overmodulation strategy. It is observed in both simulation and experimental results that the d–q-axis current responses of proposed algorithm are much faster than those of the conventional ones. In Figs. 12(c) and 13(c), $V_{\max}$ denotes a

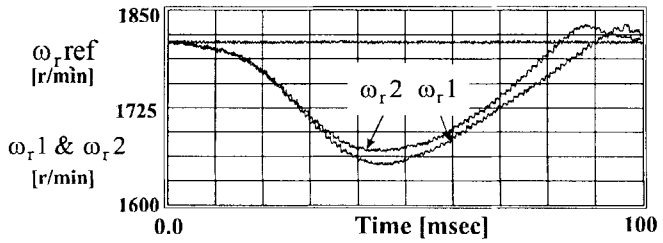

Fig. 14. Comparison of speed responses in load change. $\omega_r 1$: conventional strategy and $\omega_r 2$: proposed strategy.

magnitude of controller output-voltage vector limited by dc-link voltage. From these waveforms, all the current controllers fully use their control voltage in transient region. This means that this performance difference is only caused by the voltage-selection technique in the overmodulation region.

To compare the difference of output torque in both strategies, the speed dipping is shown in Fig. 14. Disregarding the current dynamics, the speed dipping of the conventional strategy is larger than that of the proposed one. The results show that the speed dipping of proposed strategy is reduced by 18% compared with that of the conventional one. Actually, because the ideal step load change is not straightforward by induction machine, and the test machine is connected via a flexible coupling to a load induction machine. The responses of speed dipping are somewhat different from those in simulation result. The experimental results have sufficiently verified the feasibility of the proposed overmodulation technique.

VI. Conclusions

In this paper, a novel overmodulation strategy considering the current dynamics is proposed. The current dynamics are determined by the difference between the machine terminal voltage and the machine-back EMF. Therefore, considering the machine-back EMF, the optimal inverter output voltage is selected in the proposed overmodulation strategy. With the help of a novel overmodulation strategy, required electrical torque can be directly produced as quickly as possible, and fast machine drive characteristics can be achieved even in the transient condition without considerable effort. With this overmodulation scheme on the controller, by just adding a software program, an inverter can be effectively utilized for any ac-current regulation system. The effectiveness of the proposed scheme is sufficiently verified through computer simulation and experiment.

References

[1] T. G. Habetler, F. Profumo, M. Pastorelli, and L. M. Tolbert, "Direct torque control of induction machines using space vector modulation," *IEEE Trans. Ind. Applicat.*, vol. 28, no. 5, pp. 1045–1053, 1991.
[2] G. Griva, T. G. Habetler, F. Profumo, and M. Pastorelli, "Performance evaluation of a direct torque controlled drive in the continuous PWM-square wave transition region," *IEEE Trans. Power Electron.*, vol. 10, no. 4, pp. 464–471, 1995.
[3] A. B. Plunkett, "A current-controlled PWM transistor inverter drive," in *IEEE-IAS Conf. Rec.*, 1979, pp. 785–792.
[4] J. Holtz, "Pulsewidth modulation—A survey," *IEEE Trans. Ind. Electron.*, vol. 39, no. 5, pp. 410–420, 1992.
[5] J. Holtz, W. Lotzkat, and A. Khambadkone, "On continuous control of PWM inverters in the overmodulation range including the six-step mode," in *IECON 18th Annu. Conf. IEEE Ind. Electron. Soc.*, 1992, pp. 307–312.
[6] R. J. Kerkman, D. Leggate, B. J. Seibel, and T. M. Rowan, "Operation of PWM voltage source-inverters in the overmodulation region," *IEEE Trans. Ind. Electron.*, vol. 43, no. 1, pp. 132–141, 1996.
[7] D. R. Seidl, D. A. Kaiser, and R. D. Lorenz, "One-step optimal space vector PWM current regulation using a neural network," in *IEEE-IAS Conf. Rec.*, 1994, pp. 867–874.
[8] H. Mochikawa, T. Hirose, and T. Umemoto, "Overmodulation of voltage source PWM inverter," in *JIEE Ind. Conf. Rec.*, 1991, pp. 466–471.
[9] T. M. Jahns, G. B. Kliman, and T. W. Neumann, "Interior permanent-magnet synchronous motors for adjustable-speed drives," *IEEE Trans. Ind. Applicat.*, vol. IA-22, no. 4, pp. 738–747, 1986.
[10] T. M. Rowan and R. J. Kerkman, "A new synchronous current regulator and analysis of current regulated PWM inverters," *IEEE Trans. Ind. Applicat.*, vol. IA-22, no. 4, pp. 678–690, 1986.
[11] R. D. Lorenz and D. B. Lawson, "Performance of feedforward current regulators for field-oriented induction motor controllers," *IEEE Trans. Ind. Applicat.*, vol. IA-23, no. 4, pp. 597–602, 1987.
[12] H. W. Van der Broeck and H. C. Skudelny, "Analysis and realization of a pulse width modulator based on voltage space vectors," *IEEE Trans. Ind. Applicat.*, vol. 24, no. 1, pp. 142–150, 1988.
[13] J.-K. Seok and S.-K. Sul, "A new overmodulation strategy for induction motor drive using space vector PWM," in *Proc. APEC 95*, pp. 211–216.

Jul-Ki Seok (S'94) was born in Pusan, Korea, in 1969. He received the B.S., M.S., and Ph.D. degrees in electrical engineering from Seoul National University, Seoul, Korea, in 1992, 1994, and 1998, respectively.

He is currently with SamSung Electronics Corporation, Suwon City, Kyungki-Do, Republic of Korea. His research interests are in high-performance electrical machine drives and high-power ac drives.

Joohn-Sheok Kim (S'92–M'97) was born in Korea in 1965. He received the B.S., M.S., and Ph.D. degrees in electrical engineering from Seoul National University, Seoul, Korea, in 1989, 1992, and 1995, respectively.

From 1995 to 1996, he was with the Engineering Research Center, Seoul National University. Now, he is with the University of Inchon, Inchon, Korea, as an Assistant Professor. His major interest is power electronics, especially in the area of adjustable-speed ac drives and static power converter.

Seung-Ki Sul (S'78–M'87) was born in Pusan, Korea, in 1958. He received the B.S., M.S., and Ph.D. degrees in electrical engineering from Seoul National University, Seoul, Korea, in 1980, 1982, and 1986, respectively.

He was with the Department of Electrical Engineering, University of Wisconsin, Madison, as a Visiting Research Associate from 1986 to 1988. From 1988 to 1990, he was with GoldStar Industrial Systems Company, Seoul, as a Principal Research Engineer. Since 1991, he has been a Faculty Member at the School of Electrical Engineering, Seoul National University, as an Associate Professor. His present research interests are in high-performance electric machine control, electric vehicle drives, and power converter circuits. He is performing various research projects for industrial systems, and some of the results are applied to the field of industrial high-power electric machine control.